Solar-powered ROV: advancing underwater exploration with renewable energy.

LAWAL, S.M., VALIZADEH, S., FOUGH, N. and KANNAN, S.

2024

Solar-Powered ROV: Advancing Underwater Exploration with Renewable Energy

Sani Mohammed Lawal
School of Engineering
Robert Gordon University
United Kingdom
s.lawal1@rgu.ac.uk

Shima Valizadeh
Department of Theoretical Physics and Nano
Alzahra University,
Tehran, Iran
sh.valizadeh59@gmail.com

Nazila Fough
School of Engineering
Robert Gordon University
United Kingdom
n.fough1@rgu.ac.uk

Somasundar Kannan
School of Engineering
Robert Gordon University
United Kingdom
s.kannan1@rgu.ac.uk

Abstract— **Considering the importance of remotely operated vehicles (ROVs) in conducting inspections, data collection, and exploration beneath the sea surface, this paper proposes a solar-powered ROV solution. Solar power is employed to power the ROV/AUV, with an appropriately designed solar panel providing 5 hours of performance for the Blue ROV. A miniaturized 10Hp/12kg ROV is being considered for underwater activities, with an energy demand load of 943.68W. To meet this demand, solar panels are installed on floating platforms to generate the necessary power, with meticulous calculations determining the best number and size of solar modules. In order to ensure continuous operation, inverters, charge controllers, and battery banks are sized accordingly. The proposed model optimizes silicon solar cells using the COMSOL Multiphysics environment. Simulations in COMSOL Multiphysics validate results against design parameters, confirming adherence to calculated values. The use of solar-powered systems improves operational effectiveness while also ensuring long-term sustainability in maritime activities. The solar-powered ROV represents a significant step towards environmentally conscious and efficient underwater exploration in the Gulf of Guinea and elsewhere by utilizing renewable energy.**

Keywords— ***COMSOL Multiphysics, Remotely Operated Vehicle (ROV) Solar Photovoltaic, Silicon Solar Cell, Gulf of Guinea***

I. INTRODUCTION

Remote Operated Vehicles (ROVs) play a crucial role in Africa's maritime activities, facilitating exploration, research, and resource management in its vast coastal waters. In this context, the Gulf of Guinea region stands out due to its rich marine biodiversity and untapped underwater resources and it is the case study for this work. Recognizing the significance of ROVs in this region, we propose the development of a solar powered remotely operated vehicle (ROV) to conduct inspections, data capture, and exploration beneath the sea surface. By harnessing solar energy, the proposed work aim to power ROV operations efficiently while minimizing environmental impact and reducing dependence on non-renewable energy sources.

The promise of renewable energy resources and their associated technologies offers a dependable solution for powering current and upcoming technologies. Among these renewable sources, solar energy stands out as the safest, cleanest, and most abundant form [1-3]. This study proposes solar energy as a viable energy source for remote-operated vehicles (ROVs). ROV is a device that is used for underwater adventures which is powered through an umbilical/tethering connection for both electrical energy and data transfer [4,5].

The offshore area like the Gulf of Guinea requires underwater observation of facilities and the natural resources as being conducted by humans. However, the task of carrying out this observation by humans is difficult, expensive, unsafe for workers, and time-consuming. Numeral research has brought different solar-powered remote-operated vehicles (Fig 1) as reported in[1]–[4] but there was short consideration of the specific case studies such as Gulf of Guinea in the Sub-Saharan region of Africa or most times the existing proposed models are too expensive and complex to manage.

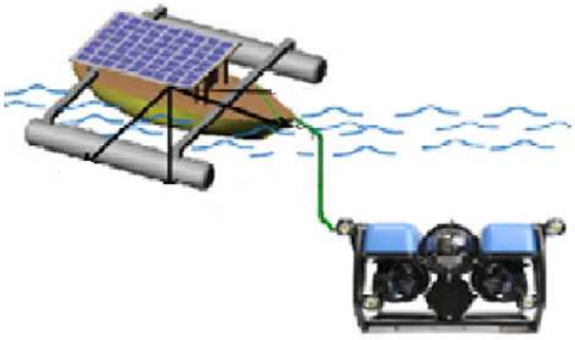

Fig 1. Solar-powered Remotely Operated Vehicle (BlueROV)[5][3]

II. CASE STUDY AREA

The Gulf of Guinea is one of the most important oceans utilized by different multinationals and is located at 0°N latitude and 0°E longitude within the Sub-Saharan and Central Africa coastlines with territorial waters of the Atlantic Ocean. The Gulf of Guinea as shown in Fig 2, is among other territorial waters that require security and safety management, among other criminal activities taking place in the region; oil bunkering from the Nigerian Niger/Delta region, there are issues of kidnappers using the sea as an escape route. Piracy and Smuggling is another type of criminal activity taking place in the Gulf of Guinea. In the Gulf of Guinea, different resources can be harnessed for economic development by the countries surrounding the

region. The average sea surface temperature in the Gulf of Guinea ranges from 27.13°C for the dry season and 22.52°C for the wet season. The Gulf of Guinea, being in the Sub Sahara African region is blessed with solar irradiance of an average range of 5.1MJ/m^2/day to 13.1MJ/m^2/day[6][7]

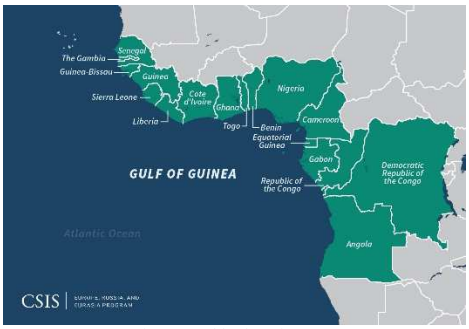

Fig 2, Gulf of Guinea[8]

Remote-operated underwater vehicles can be used for different purposes underwater such as site inspections, surveillance, monitoring, exploration, scientific research, search and recovery, and industrial research due to their ability to explore, data capture, and storage. However, the ROV requires energy to carry out the assigned task. Electrical devices operate based on their electrical power consumption which depends on the size and the task to be accomplished. The solar-powered ROV encompasses various components, including the propulsion system, payload capacity, communication equipment, battery, control system, and solar panels. The proposed model optimizes silicon solar cells material using the COMSOL Multiphysics environment, even though other type material such as in [9] can be used.

III. METHODOLOGY

The solar energy available in the Gulf of Guinea adheres to several parameters such as the temperature of the site as mentioned by the National Aeronautics and Space Administration (NASA)[7]. The ROV considered in this work is the mini blueROV2 [14] with a maximum weight size of 12kg with a power rating of 10Hp, and this ROV can go up to 300 meters under the sea. The subsequent subsections assess the estimation of energy demand by BlueROV, mathematical modeling of floating PV, selection and sizing of elements, capacity sizing of the battery bank, sizing of the inverter capacity, sizing of the charge controller, and sizing of the cables.

A. Energy Demand Estimation

The total energy demand of the various components in the ROV is estimated based on their power ratings to determine the total wattage required daily with respect to operational hours. Table 1 presents the summary of the loads with the total power to be used as 4,675 Watt-hour per day and indicate the total peak load as 935W.

B. Mathematical Modeling of Floating PV

Since the solar PV will be installed on a floating surface, therefore, the sea wind speed (V_{ws}) and the sea temperature (Tw) need to be used to determine the cell temperature of the floating solar PV system that will be powering the ROV[10][8], [9],10]. Using sea temperature and land (Air) temperature relationship, as in:

$$T_w = 5 + 0.75T_{air} \quad (1)$$
$$= 5 + 0.75(27.65) = 25.74^oC,$$

where:
T_w – Sea temperature
T_{air} – Air temperature

However, due to the cooling influence of the water, the water temperature decreases as it reacts, as shown by the coefficients of the formula. As can be seen in the relationship above, the sea (water) temperature will rise as the air (wind) temperature is less than 20^{o}C[13], [14]. Therefore, using the relation in (2)

$$V_{ws} = 1.62 + 1.17\ x\ V_{wl}\ , \quad (2)$$

where:
V_{ws} – Sea wind speed
V_{wl} – Land wind speed

The wind speed in terms of velocity on the sea is constantly higher than that of the land, i.e the wind velocity (Vws) on the sea surpasses the wind velocity (Vwl) over the land[15] Therefore,

$$V_{ws} = 1.62 + 1.17\ x\ 9.16 = 12.34m/s$$

TABLE 1 SUMMARY OF THE LOADS [3], [5], [16], [17]

S/N	Load	Qty	Power Rating (W)	Hours /day	Peak load (W)	Daily Use (Wh/day)
1	Electric motor	2	75	5	150	750
2	Lights	4	10	5	40	200
3	HD Camera	1	10	5	10	50
4	Sensor	3	1	5	3	15
5	Acoustic Modem	1	5	5	5	25
6	Wi-Fi Modem	1	5	5	5	25
7	Thruster Propeller	4	65	5	260	1300
8	Motor Controller	4	65	5	260	1300
9	Micro controller	1	2	5	2	10
10	Sonar	1	200	5	200	1000
	Total				**935**	**4675**

C. Determination of the solar cell temperature both on the sea and land

Solar PV Cell Temperature on land is given by [18], as in:

$$T_c = (0.943\ x\ T_{air}\ ) + (0.0195\ x\ G) - (1.528\ x\ V_{wl} + 0.3529, \quad (3)$$

where:
T_c – Land cell temperature in ^{o}C
G – STC irradiation (1000W/m^2)

$$T_c = (0.943\ x\ 27.65) + (0.0195\ x\ 1000) - (1.528\ x\ 9.16 + 0.3529$$

$$= (27.09) + (19.5) - (13.996) + 0.3529 = 32.24^{o}C$$

Solar PV Cell temperature on the sea is given by [15] as in:

$$T_{cw} = (0.943\ x\ T_w) + (0.0195\ x\ G) - (1.528\ x\ V_{ws} + 0.3529) \quad (4)$$

Where; T_{cw} - Sea cell temperature in ^{o}C
T_w – Sea temperature in ^{o}C
V_{ws} – Sea wind speed in m/s
G –STC irradiation (1000W/m^2)

$$T_{cw} = (0.943\ x\ 25.74) + (0.0195\ x\ 1000) - (1.528\ x\ 12.34 + 0.3529) = 24.2728 + 19.5 - 18.8555 + 0.3529 = 24.56^{o}C$$

D. Sizing of the floating Solar PV for the ROV

The performance of the solar PV array is influenced by the de-rating factors that impact the solar PV, these factors include dirt, temperature, and mismatches. The daily energy output power for the PV array can be determined by Equation (5) as suggested in [19]–[21].
The photovoltaic array produces DC electricity in direct proportion to the global solar radiation.

$$\text{Ppv-array} = \frac{EL}{\frac{G}{(G_{STC})} + \left(\frac{fDC}{AC}\right) + ftemp} \quad (5)$$

where:
EL – Estimated Load for energy required per day (Wh/day)
FDC/AC DC to AC with de-rating factor (%) = 0.778
Ppv-array – The array of solar Photovoltaic
β - Temperature coefficient of max. Power (%/^{o}C) = -0.38%
G – Solar radiation incident on PV array in kW/m^2
G_{STC} – Incident radiation under STC of 1kW/m^{2}or 1000W/m^2
Tc – PV cell temperature in current time step (^{o}C)

TSTC – PV cell temperature under STC, TSTC = 25 ^{o}C

Given that; $F = 1 - \beta(T_{cw} - TSTC)$

E. Sea PV installation

Factors such as PV cell temperature under STC and Sea cell temperature need to be considered before the sea PV installation.

$$F = 1 - \beta(T_{cw} - TSTC) \quad (6)$$

F_{temp}= 1 – [-0.38% (24.56– 25)] = 0.998
G = Solar radiation incident on PV = 6.38 kWh/m^2[7]
G_{STC} = Solar incident radiation under STC of 1kW/m^2

Therefore,
PPV-Array = $\frac{4675}{\frac{6.38}{1}\ x\ (0.778) x\ 0.998}$ = 943.68W (The total power in the PV array)

The recommended system voltage is 48 V dc based on Sandia's Handbook recommendation [22]. The ENP Sonne High Quality 180 Watt, 24V monocrystalline module is selected in this work. It has a short circuit current (Isc) of 5.38A, panel efficiency of 14.1%, and power temperature coefficient of -0.480 %/^{o}C[23].

F. Determination of the number of modules connected in series.

Since 48V system voltage is selected, modules to be connected in series can be determined as follows:

$$N_{ms} = \frac{V_{system}}{V_{module}} \quad (7)$$

where:
N_{ms} – Number of modules in series
V_{system}– System Voltage
V_{module} – Module Voltage

$$N_{ms} = \frac{48}{24} = 2 \text{ modules}$$

The number of modules connected in parallel is given as in (8):

$$N_{mp} = \frac{P_{pv-array}}{N_{ms} + P_{module}} \quad (8)$$

$$N_{mp} = \frac{943.68}{2 + 180} = 5.19 = 6$$

The total number of modules required to generate 4,675 Wh/day power is as follows.

$$N_{mt} = N_{ms}\ \text{X}\ N_{mp} \quad (9)$$

where:
N_{mt} = Number of total modules required
= 2 x 6 = 12 modules

G. Battery Bank Capacity Sizing

The battery bank capacity required (Cx) can be calculated as in:

$$C_x = \frac{N_c + E_L}{DoD_{max}\ x\ V_{system}\ x\ \eta_{out}}, \quad (10)$$

where:
C_X = Required battery capacity in Ampere-hour (Ah)
N_C = Number of days of autonomy = 3 days
EL = Estimated load Energy in Wh = 4675Wh
DoD_{max} = Maximum Depth of Discharge = 80% (0.8)
η_{out} = Output efficiency

$$\eta_{out} = \eta_{bat}\ \text{x}\ \eta_{inv} \quad (11)$$

Where:
η_{bat} = 0.85
η_{inv} = 0.985

η_{out} = 0.85 x 0.985 = 0.84

Therefore, the required battery capacity:

$$C_x = \frac{3 + 4675}{0.8\ x\ 48\ x\ 0.84} = 145.027 \text{ Ah}$$

A lithium-ion battery 14.8V 18Ah with a high capacity, light in weight, and suitably enclosed, mainly designed for

blueROVs usage is selected for this work[5]. The number of batteries required to be calculated as follows:

$$N_{Breq} = \frac{C_x}{C_{selected}} = \frac{145.027}{18} = 8.06 = 9 \quad (12)$$

The number of batteries in the series is as follows.

$$N_{Bs} = \frac{V_{system}}{V_{battery}} = \frac{48}{14.8} = 3.24 = 4 \quad (13)$$

The number of batteries in parallel is as follows.

$$N_{Bp} = \frac{N_{Breq}}{N_{Bs}} = \frac{9}{4} = 2.25 = 3 \quad (14)$$

The total number of batteries required for the system is calculated based on (15). Therefore;

$$TN_{bS} = N_{bp} \text{ x } N_{bs} = 4\ x\ 3 = 12\ batteries \quad (15)$$

H. Inverter Capacity Sizing

In determining the size of the inverter, the initial step is to identify the actual total sum of power consumption by the loads that operate simultaneously. In this work for instance 50% of the total loads. Due to the high starting current of large electric motors, a factor of 3 is being considered to multiply their power[20] Also, for system expansion, the sum of the individual peak loads value is being multiply by 1.25 as a safety factor[24], [25]

$$P_{inv} = PRS\ X\ 1.25, \quad (16)$$

where:
P_{inv} - Inverter Power Rating
PRS - Power of appliances running simultaneously.

$$P_{inv} = 935\ X\ 1.25 = 1{,}168.75W$$

Based on the calculated value (1,168.75W), a 1.2kW inverter is selected with a 48v nominal voltage.

I. Charge Controller Sizing

The rated current of the regulator is as follows:

$$I_{rated} = N_{mp} \text{ x } I_{sc} \text{ x } F_{safety} = 6 \text{ x } 5.38 \text{ x } 1.25 = 40.35A, \quad (17)$$

where:
N_{mp} - Number of modules in parallel
I_{sc} - Module short circuit current = 5.38A
F_{safety} – Safety factor = 1.25

Solar Charge Controller 48v 80A
Number of charge controllers required is as follows:

$$N_{ccreq} = \frac{I_{rated}}{I_{selected}} = \frac{40.35}{80} = 0.50 = 1 \quad (18)$$

J. Cable Sizing

In the selection of the appropriate size and type of cable, careful consideration must be applied because it enhances performance and brings about the reliability of the system. Current flows through cable from solar PV to the charge controller I_{cab} is equal to the rating of the charge controller[26]

$$A = \frac{PLI_{rated}}{V_d}\ x\ 2 = \frac{1.724\ x\ 10^{8}\ x\ 10\ x\ 80}{48\ x\ 0.04}\ x\ 2 = 1.437x10\text{^}{-5} = 14.37x10\text{^}{-6} \quad (19)$$

Therefore, 16mm is being proposed based on the calculated value.
p - The resistivity of the copper conductor selected for the system is taken as 1.724 x 10-8
L - Length of the conductor (10m)

In standalone wiring for solar photovoltaic systems, the voltage drop is taken not to exceed 4%. Therefore, a cable with a 16mm^2 cross-sectional area is selected[27].

IV. Modeling in COMSOL Multiphysics Environment

The COMSOL Multiphysics software uses the Finite Element Method to solve continuity equations as in (20) while simulating solar cells, this is to eliminate the issue of non-uniform illumination on the surface of the solar cell and, to find the current density distribution.

$$-\nabla.(\sigma\nabla V - ȷ) = Q, \quad (20)$$

where V is the electric potential, $ȷ$ is the current density, Q is the generated current and σ is the conductivity of the material.

The generated current density is presented in (21) while the governing equation in solving continuity equation (20) using the Finite Element Method.

$$G = j_1 G + j_2 T^3 \exp\left[\frac{-E_g}{k_g T}\right]\left(\exp\left[\frac{V_j}{nV_T}\right] - 1\right) + j_3 V_j \quad (21)$$

In the modeling of a Photovoltaic (PV) array, some parameters are considered such as open circuit voltage (V_{oc}), short circuit current (I_{sc}), Maximum Power Point (MPP), the efficiency of the solar cell, and the fill factor. Using the one-diode model as represented in Fig. 3, the total current flowing into the load resistance RL is presented in equations (22) & (23)[28] where I_{ph} and I_d are the photo-generated current and diode current respectively.

$$I = I_{ph} - I_d \quad (22)$$

$$I = I_{Ph-}\ I_O\left[\exp\left[\frac{V}{nVT}\right] - 1\right] - \frac{V_j}{R_{sh}} \quad (23)$$

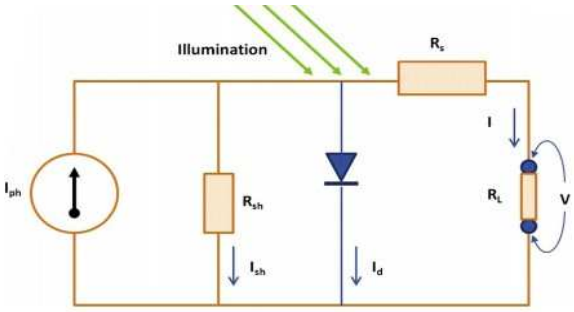

Fig 3. PV Cell Equivalent Circuit

The V_t represents the thermodynamic voltage, V_j is the junction voltage, K_B is the Boltzmann constant, q_e is the electron change while n is the ideality factor.

$$V_T = K_B T/q_e \quad (24)$$

$$V_j = V + IR_e \quad (25)$$

The general form of current generated by a solar cell is presented in (23) but can be reduced based on the type of emitter region I_e and the finger regionI_{da}. Also, the photo-generated current depends on the level of illumination, which is directly proportional to its intensity[29]. COMSOL Multiphysics software was used for the modeling and simulation even though other software available such as in [30]. The software was employed because of its versatility in nature and ability to solve numerical problems in different dimensions. In this work, 2D dimensional has been used for the numerical solutions as presented in Fig. 4.

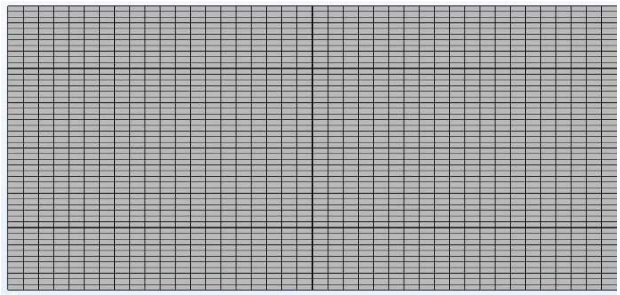
Fig 4. Model of Solar PV Cells Array in COMSOL

The modeling started with a single silicon solar cell, gradually increasing to reach the total number of cells in a module and moving to modules in an array as indicated in Figure 4. Figure 5 shows the sequence of the solar cell modeling and simulation based on the required number of modules as calculated in equation (9).


Fig 5. Single Solar Cell to PV Cells Array

V. SIMULATION RESULTS USING COMSOL MULTIPHYSICS

Having considered the Standard Test Condition (STC), the output simulation results show a Power output of 945.45W with an Open circuit voltage (V_{oc}) = 0.66V based on the number of solar cells therein at a maximum power point tracking (MPPT), as indicated in Fig 7. The simulated solar PV cells model (Fig 6) shows surface distribution of Incident radiation. The total power output of the PV solar cells in an array is indicated in the P-V curve as shown in fig 7.

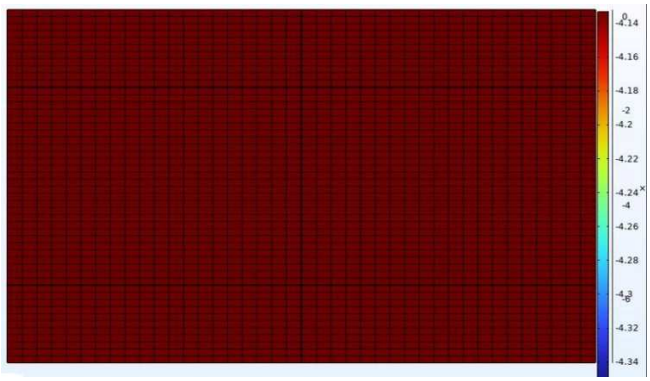
Fig 6. Simulated Solar PV Cells Arrays

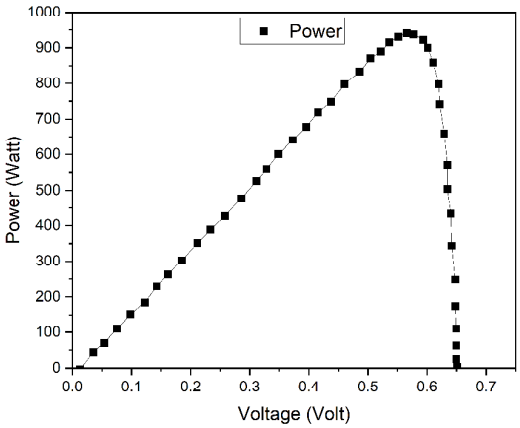

Fig 7. Power-Voltage Curve

VI. CONCLUSION

The paper has presented a solar-powered remote-operated underwater vehicle. The cumulative electrical energy demand of 943.68W has been generated by the floating offshore solar PV modules as shown in Fig 7, after the model simulation as shown in Fig 6. The paper has presented but efficient way of powering ROVs using solar PV systems that are connected in series-parallel while floating on the sea located at The Gulf of Guinea. It is designed to meet the blueROV energy requirement. The result shows the Solar PV Array can generate the required kWp for the ROV and this result has been validated with COMSOL Multiphysics Software to

verify and ensure that the proposed design will be suitable and meet up with the load demand of the ROV. The performance of solar depends on weather conditions either on land or on the sea, where floating photovoltaics are installed. These operational parameters include temperature and wind speed.

REFERENCES

.[1] I. González-Reolid, J. C. Molina-Molina, A. Guerrero-González, F. J. Ortiz, and D. Alonso, "An autonomous solar-powered marine robotic observatory for permanent monitoring of large areas of shallow water," Sensors (Switzerland), vol. 18, no. 10, pp. 1–24, 2018, doi: 10.3390/s18103497.

[2] M. D. Ageev and D. R. Blidberg, "Current progress in the development of a Solar Powered Autonomous Underwater Vehicle (AUV)," UT 1998 - Proc. 1998 Int. Symp. Underw. Technol., pp. 145–149, 1998, doi: 10.1109/UT.1998.670079.

[3] F. García-Córdova and A. Guerrero-González, "Intelligent navigation for a solar powered unmanned underwater vehicle," Int. J. Adv. Robot. Syst., vol. 10, pp. 1–13, 2013, doi: 10.5772/56029.

[4] J. R. Higinbotham, J. R. Moisan, C. Schirtzinger, M. Linkswiler, J. Yungel, and P. Orton, "Update on the development and testing of a new long duration solar powered autonomous surface vehicle," Ocean. 2008, 2008, doi: 10.1109/OCEANS.2008.5152048.

[5] "Blue Robotics - Underwater ROVs, USVs, Thrusters and Sonars!" https://bluerobotics.com/ (accessed Mar. 02, 2024).

[6] O. A. Nathaniel, A. S. Oluwadara, O. A. Joshua, and A. A. Jacob, "Estimation of Global Solar Radiation and Clearness Index in Coast of Gulf of Guinea, Nigeria," Iran. J. Energy Environ., vol. 10, no. 3, pp. 211–215, 2019, doi: 10.5829/ijee.2019.10.03.08.

[7] NASA POWER, "POWER Data Access Viewer," Nasa, 2022. https://power.larc.nasa.gov/data-access-viewer/ (accessed Mar. 03, 2024).

[8] P. Morcos, "A Transatlantic Approach to Address Growing Maritime Insecurity in the Gulf of Guinea," Cent. Strateg. Int. Stud., pp. 1–5, 2021, [Online]. Available: https://www.csis.org/analysis/transatlantic-approach-address-growing-maritime-insecurity-gulf-guinea.

[9] S. Valizadeh, A. Shokri, A. Sabouri-Dodaran, N. Fough, and F. Muhammad-Sukki, "Investigation of efficiency and temperature dependence in RbGeBr3-based perovskite solar cell structures," Results Phys., vol. 57, no. January, p. 107351, 2024, doi: 10.1016/j.rinp.2024.107351.

[10] A. Tim Umoette, "Design of Stand Alone Floating PV System for Ibeno Health Centre," Sci. J. Energy Eng., vol. 4, no. 6, p. 56, 2016, doi: 10.11648/j.sjee.20160406.12.

[11] D. F. Al Riza and S. I. U. H. Gilani, "Standalone photovoltaic system sizing using peak sun hour method and evaluation by TRNSYS simulation," Int. J. Renew. Energy Res., vol. 4, no. 1, pp. 109–114, 2014.

[12] J. Suh, Y. Jang, and Y. Choi, "Comparison of electric power output observed and estimated from floating photovoltaic systems: A case study on the hapcheon dam, Korea," Sustain., vol. 12, no. 1, 2020, doi: 10.3390/su12010276.

[13] S. T. Mohammad, H. H. Al-Kayiem, M. A. Aurybi, and A. K. Khlief, "Measurement of global and direct normal solar energy radiation in Seri Iskandar and comparison with other cities of Malaysia," Case Stud. Therm. Eng., vol. 18, no. January, p. 100591, 2020, doi: 10.1016/j.csite.2020.100591.

[14] D. J. McCafferty, C. Gilbert, A. M. Thierry, J. Currie, Y. Le Maho, and A. Ancel, "Emperor penguin body surfaces cool below air temperature," Biol. Lett., vol. 9, no. 3, pp. 2–5, 2013, doi: 10.1098/rsbl.2012.1192.

[15] J. Siecker, K. Kusakana, and B. P. Numbi, "A review of solar photovoltaic systems cooling technologies," Renew. Sustain. Energy Rev., vol. 79, no. July 2016, pp. 192–203, 2017, doi: 10.1016/j.rser.2017.05.053.

[16] I. Patiris, "Remote Operated Vehicle (ROV)," Encycl. Ocean Eng., pp. 1456–1456, 2022, doi: 10.1007/978-981-10-6946-8_300645.

[17] R. Capocci, G. Dooly, E. Omerdić, J. Coleman, T. Newe, and D. Toal, "Inspection-class remotely operated vehicles-a review," J. Mar. Sci. Eng., vol. 5, no. 1, 2017, doi: 10.3390/jmse5010013.

[18] A. M. Muzathik, "Photovoltaic Modules Operating Temperature Estimation Using a Simple Correlation," Int. J. Energy Eng., vol. 4, no. November, pp. 151–158, 2014.

[19] G. E. Ahmad, "Photovoltaic-powdered rural zone family house in Egypt," Renew. Energy, vol. 26, no. 3, pp. 379–390, 2002, doi: 10.1016/S0960-1481(01)00131-8.

[20] M. Ishaq, U. H. Ibrahim and H. Abubakar, "Design Of An Off Grid Photovoltaic System: A Case Study Of Government Technical College, Wudil, Kano State," International of Journal of Technology Ehancments and Emerging Engieering Reseach, 2(12), pp. 175–181, 2013,

[21] Council, "Clean Energy Council," Grid-Connected Sol. PV Syst. Des. Guidel. Accredit. Install., no. January, pp. 1–18, 2013.

[22] Sandia National Laboratories, "Stand-Alone Photovoltaic Systems: A Handbook of Recommended Design Practices," Absorpt. Fluids Data Surv. Final Rep. Foreign Data, pp. 1–437, 1995.

[23] E. N. P. Sonne "High Quality 180Watt 24V Monocrystalline Panel in Pallet."http://www.posharp.com/enp-sonne-high-quality-180watt-24v-monocrystalline-panel-in-pallet-p124.aspx (accessed Mar. 03, 2024).

[24] S. M. Ismael, S. H. E. Abdel Aleem, A. Y. Abdelaziz, and A. F. Zobaa, "State-of-the-art of hosting capacity in modern power systems with distributed generation," Renew. Energy, vol. 130, pp. 1002–1020, 2019, doi: 10.1016/j.renene.2018.07.008.

[25] A. Abu-Jasser, "A Stand-Alone Photovoltaic System, Case Study: A Residence in Gaza," J. Appl. Sci. Environ. Sanit., vol. 5, no. 1, pp. 81–91, 2010.

[26] B. Z. Taye, A. H. Nebey, and T. G. Workineh, "Design of floating solar PV system for typical household on Debre Mariam Island," Cogent Eng., vol. 7, no. 1, 2020, doi: 10.1080/23311916.2020.1829275.

[27] C. O. Okoye, O. Taylan, and D. K. Baker, "Solar energy potentials in strategically located cities in Nigeria: Review, resource assessment and PV system design," Renew. Sustain. Energy Rev., vol. 55, pp. 550–566, 2016, doi: 10.1016/j.rser.2015.10.154.

[28] H. Baig, N. Sellami, and T. K. Mallick, "Performance modeling and testing of a Building Integrated Concentrating Photovoltaic (BICPV) system," Sol. Energy Mater. Sol. Cells, vol. 134, pp. 29–44, 2015, doi: 10.1016/j.solmat.2014.11.019.

[29] H. Baig, N. Sellami, D. Chemisana, J. Rosell, and T. K. Mallick, "Performance analysis of a dielectric based 3D building integrated concentrating photovoltaic system," Sol. Energy, vol. 103, pp. 525–540, 2014, doi: 10.1016/j.solener.2014.03.002.

[30] S.M. Lawal, N. Fough, N. Sellami and F. Muhammad-Sukki, "Modeling and Simulation of Heterojunction Solar Cell; Determination of Optimal Values", 21st IEEE Interregional NEWCAS Conference (NEWCAS) (pp. 1-2). IEEE, 2023.